Prediction of Radiated Emissions From DC Motors

Candace R. Suriano
University of Dayton
College Park
Dayton, OH 45469 USA

John R. Suriano
ITT Automotive
2040 Forrer Blvd.
Kettering, OH 45420 USA

Gary Thiele
University of Dayton
College Park
Dayton, OH 45469 USA

Thomas W. Holmes
ITT Automotive
2040 Forrer Blvd.
Kettering, OH 45420 USA

Abstract: DC motors are known sources of radio frequency electromagnetic noise produced by arcing at the motor brushes. A simplified model of electromagnetic radiation from a DC motor and associated wiring harness is introduced and compared to measurements. This model relates motor arc characteristics to the radio frequency emissions of the motor and wiring circuitry which can be used to guide engineers in the design process. This technique is intended to form the basis for a motor design aid.

INTRODUCTION

By the nature of their operation DC motors are notorious sources of RF emissions. Radiation at a fixed frequency from a typical small DC motor is shown in Figure 1. This particular motor has ten commutator bar segments and should undergo ten distinct arcing event cycles during one revolution. As can be seen in the trace, there are twenty distinct regularly spaced events during a single revolution of the armature. A single commutation cycle has two transient spikes either because of lack of synchronism in the commutation from the two brushes or because one set of spikes represents the start of commutation and the other the end of commutation. Commutation arcing results in broadband coherent noise which can impact a variety of electronic systems.

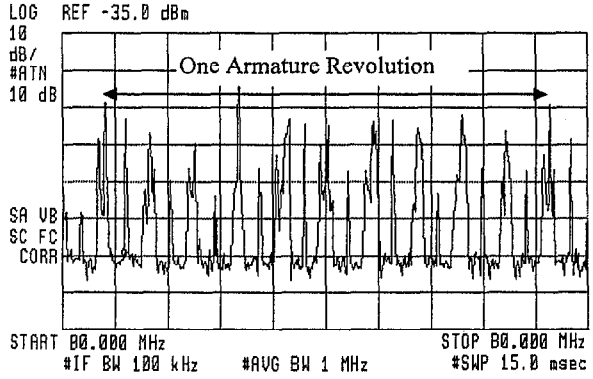

Figure 1. Trace of DC Motor Radiation at Fixed Frequency

Previous studies have characterized the conditions that are present during commutation [1-3] and have examined the arcing using empirical methods [4-6]. Studies of radio frequency noise have been limited to empirical studies [7] and predictions of conducted emissions [8]. This study examines the radiated emissions using simplified mathematical models of the commutation process, the arcing characteristics, and the radiation characteristics of the motor and wiring harness. Suppression components for filtering RF emissions can also be included in the model.

This model incorporates three stages as shown in Figure 2. The motor/commutation model determines the arc duration from a time domain solution of the motor electrical equations. A fourier transform of the arc voltage is supplied to the radio frequency model where it is used with an impedance model of the wiring harness to compute common mode current from the motor. The common mode current is used with a simple monopole antenna model of the wiring harness to predict the radiation intensity. This study explains the mechanisms by which DC motors radiate RF noise, the relationship of design parameters to the noise, and is useful for optimization of both the motor and suppression circuitry.

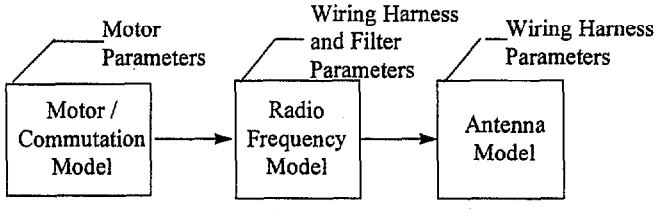

Figure 2. Block Diagram of Motor Radiation Model Stages

COMMUTATION MODEL

Arcing between brushes and commutator bars in a DC motor provides a broadband forcing function which results in radiated emissions from the motor. To predict the duration of the arc which exists during the period of abrupt current reversal, this study utilizes a numerically solved time domain circuit network model similar to [2]. This model includes information on the motor design and operating conditions. Modifications to the motor design impact the solution of the commutation current and the arc characteristics, and hence the radiated noise.

An initial steady state current level is determined based on the emperical and theoretical parameters of the DC motor. This provides the initial condition which is used to calculate the currents when the motor begins commutating as shown in

0-7803-5015-4/98/$10.00 © 1998 IEEE

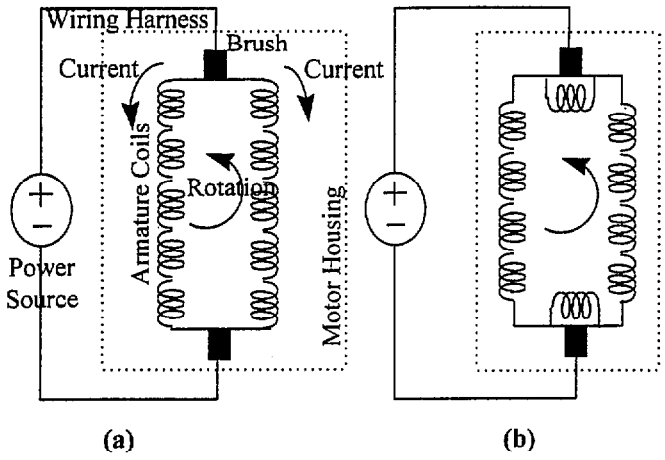

Figure 3. DC Motor (a)Prior to Commutation (b) Commutating

Figure 3(a) and 3(b). Before commutation the current splits between parallel paths in the motor winding as in Figure 3(a). During commutation, one of the coils in each series in the motor is shorted prior to reversal of the current in that coil. Ideally, the current in the shorted coil reverses during the time it is shorted due to the back EMF induced in the coil from the magnets. When the current in the shorted coil does not reverse, energy stored in the coil causes the current to continue as commutation ends. Thus the arc is struck as shown in Figure 4 allowing continuity of current in the commutating and non-commutating coils. The arc is extinguished as the current in the shorted coil reverses.

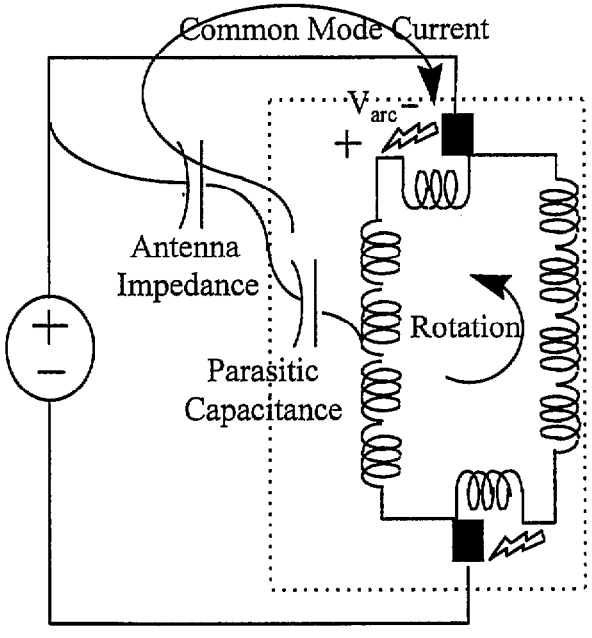

Figure 4. Commutation Arc and Common Mode Current.

The arc condition shown in Figure 4. results in radiation from the motor. The voltage present at the arc, produced by the inductive voltage of the motor windings, excites the wiring harness with a high frequency pulse resulting in common mode current. The current returns via parasitic capacitance between the armature and motor case and between the motor case and the wiring harness. This common mode current results in radiation from the motor wiring harness.

The characteristics of the arc used in the model have been taken from the literature [5,9] and from test data. Measurement of brush arcing is shown in Figure 5. For convenience, the brush was lifted from the commutator in order to draw an arc in this test. The arc has a nearly constant voltage of approximately 15V. The arc is actually a nonlinear resistance which constrains the voltage from the inductive load. The arc resistance, deduced from voltage and current, is shown in Figure 5 as well. For the radio frequency model of the motor the motor noise source is modeled as a voltage (the arc voltage) in series with a source resistance (the arc resistance).

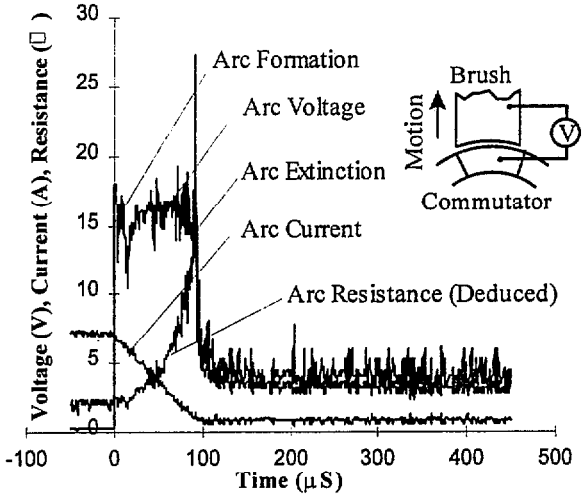

Figure 5. Arc Voltage Measured Under Static Conditions.

For this study two types of arcs were considered. Constant voltage, as suggested by Figure 5, and a two stage arc starting with constant voltage and ending with constant E-field at the brush edge. As described in [9], if the arc does not terminate before a certain separation distance is attained between contacts, the arc voltage will rise to maintain the E-field at an approximately constant level until the current is extinguished. It is possible that the tests of Figure 5 could not achieve this condition with the relatively low separation velocity that was used, and hence this effect is not seen.

RADIO FREQUENCY MODEL

The arc voltage is a broadband forcing function for the motor's wiring harness acting as an antenna much as the spark gap generators of Marconi's transmitters [10]. To compute the

broadband radiation from the wiring harness it is necessary to determine the frequency spectrum of the arc. For the simplified arc models shown in Figure 6 it is a simple matter to compute the single sided Fourier transforms. The continuous transforms are used since the period of the commutation pulses is typically hundreds of hertz, orders of magnitude less than the resolution bandwidth (RBW) of the typical EMC test. Thus, rather than summing spectral lines within the RBW of a particular frequency, the signal is treated as continuous. At any given frequency the magnitude is adjusted by a bandwidth correction factor by assuming that the signal level is constant within the receiver bandwidth.

The single sided Fourier transform of the constant voltage arc shown in Figure 6(a) at a frequency f is a well known result,

$$V_{ARC}(\omega) = 2T_A V_A \frac{\sin(\pi f T_A)}{\pi f T_A}. \quad (1)$$

While the transform of the constant E-field arc shown in Figure 6(b) at a frequency f is easily obtained:

$$V_{ARC}(\omega) = \frac{1}{2\pi^2 f^2}\frac{V_A - V_E}{T_E - T_A}\left[e^{-j2\pi f T_A} + je^{-j2\pi f T_E}\left(2\pi f(T_A - T_E) + e^{j\frac{\pi}{2}}\right)\right] + \frac{V_A}{2\pi f}e^{j\frac{\pi}{2}}\left(e^{-j2\pi f T_E} - 1\right) \quad (2)$$

When computing the common mode current using either (1) or (2), it is also necessary to incorporate the effects of the arc resistance in series with the arc voltage as shown in Figure 7. Without incorporating the arc resistance into the equations, the radiated emission level is off by 30 to 40 dB between 1 MHz and 1GHz. Unfortunately, there is no simple means of incorporating the arc resistance into the calculations. For the constant voltage arc, typical arc resistance is the same or less than the impedance of the harness and parasitic capacitance. However, for the constant E-field arc the resistance can be very large. Without incorporating the resistance, the very high voltages attained create very unrealistic currents. It was determined that using the peak resistance for both types of arcing provides suitable results as will be illustrated later.

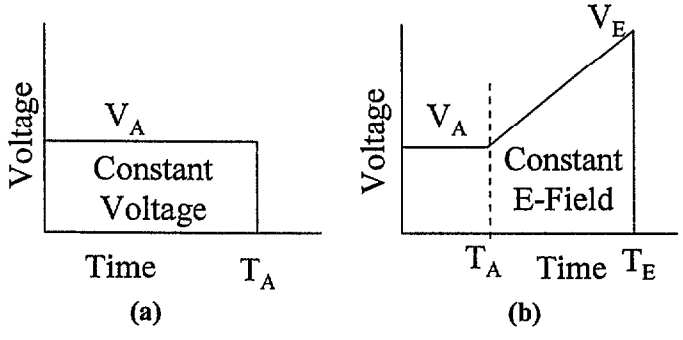

Figure 6. Constant Voltage (a), Constant E-Field (b) Arcs

ANTENNA MODEL

The motor wiring harness acts as an antenna fed by the arc as illustrated in Figure 7. The motor case, although limited in size, acts as a ground plane. The arc voltage and resistance are used with the impedance of the wiring harness and parasitic capacitance to compute the common mode current as shown in Figure 4. An approximate antenna impedance for a monopole antenna given in [11] was used for this purpose.

Knowing the common mode current it was possible to predict the radiation from the motor. The motor case forms a pseudo-ground plane for the monopole, connected to the arc source via parasitic capacitance as shown in Figure 4. Measurement of this capacitance indicate that it is on the order of 100pF. A classic near field monopole antenna model [11] was used to represent this structure.

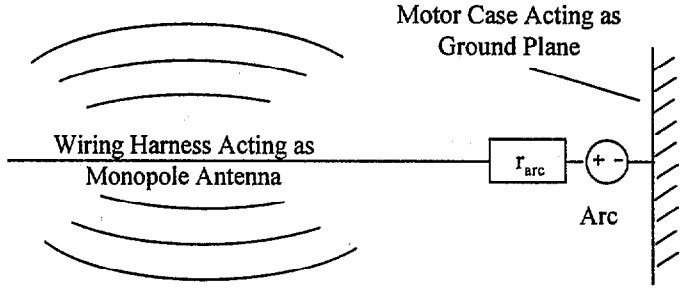

Figure 7. Grounded Monopole Approximation of Motor Wiring.

This model of the motor structure explains the rationale for the typical suppression circuitry found in small DC motors. A low pass filter placed on the leads and connected to the motor case, as illustrated in Figure 8(a), is sufficient to dramatically reduce radiation. The model can be configured as in Figure 8(b) with only one branch of the circuit, because it is unlikely that more than one brush will arc at the same instant. If both brushes should arc simultaneously, this would only increase the radiated emissions by 6dB. This model can include such a suppression circuit and thus can be used to evaluate the proper component values.

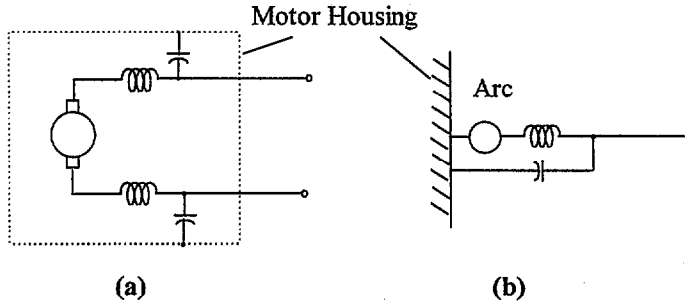

Figure 8. Typical Suppression (a), Model (b)

CASE STUDY

A fractional horsepower DC motor for an automotive application was modeled. This motor operates from the standard 12V automotive electrical supply. The motor has ten commutator bars as previously discussed. The motor has a terminal resistance of about 0.46Ω, a torque constant of about 0.026Nm/A, and a terminal inductance of about 670μH. For this study the motor was loaded to just under 12% of available stall torque, a load equivalent to that required by a typical application. The motor was tested in a semi-anechoic chamber using standard antennas, current probes, and spectrum analyzer. The motor was connected to a battery through a 3m harness. The motor was placed on a wooden bench 1m from the floor of the chamber. Since the battery was on the floor of the room a portion of the wiring harness from the battery to the table top was vertical in orientation while the remainder, approximately 1.85m was in the horizontal orientation.

Verification of Antenna Model

As confirmation of the model premise, the common mode current was recorded using an RF current probe. Peak measurements of the current and radiated field were recorded within select frequency bands using peak detection mode. The test set-up generally but not exclusively used a 10kHz band-width for measurement. The common mode current measurements were then used with the near-field monopole antenna equation to predict the radiated electric field 1m from the harness. This calculated E-field is shown in comparison to the measured E-field in Figure 9. The calculations assume a wiring harness length of 1.85m, the horizontal portion of the wire. The similarity of the two curves confirms that it is likely that the radiation is due to common mode current on the wiring harness. It also shows that the wiring harness and motor housing can be modeled successfully as a monopole antenna above a ground plane, except perhaps at the lower frequencies.

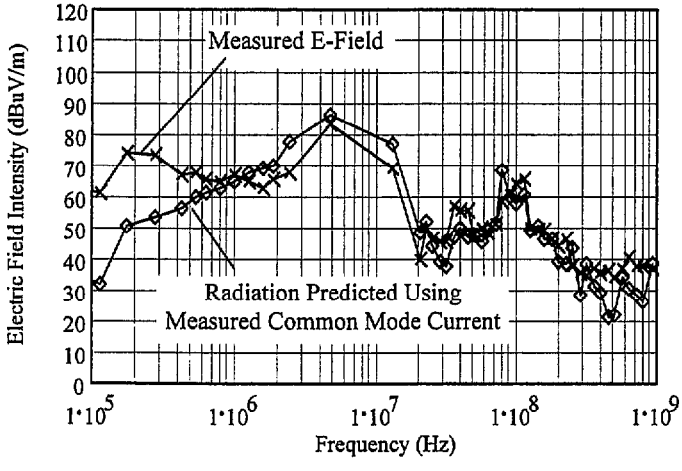

Figure 9. Radiation Predicted from Measured Current

Calculation of Arc Voltage

In order to compute the common mode current, and hence the radiation it was first necessary to predict the arc voltage. Using a time domain solution of the motor electrical circuit [2], the coil current during commutation was solved. The numerical solution was done once for the constant voltage type of arc and once for the constant E-field arc as previously described. The constant voltage arc was set at 15V, while the constant E-field was 50MV/m. The resulting arc wave-forms are shown in Figure 10, their spectrum in Figure 11. The constant voltage arc shown in Figure 10(a) lasts about 9 times longer than the constant E-field arc shown in Figure 10(b). The peak arc resistance for the constant E-Field arc is much higher, about 4300 Ohms.

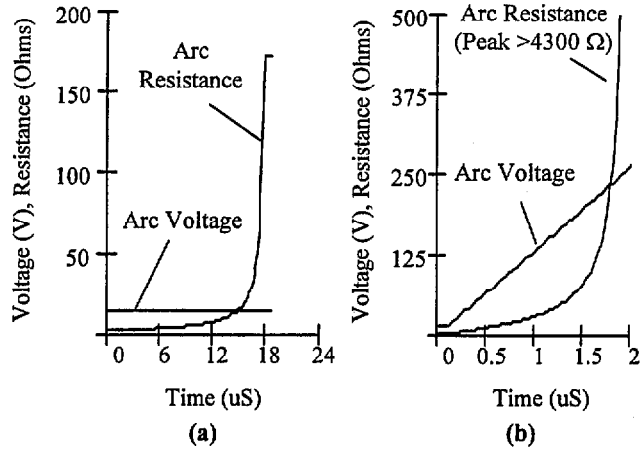

Figure 10. Constant Voltage Arc (a), Constant E-Field Arc (b).

The spectrum of each arc exhibits a characteristic 20dB/decade roll-off as shown by the plots of the Fourier transforms of each in Figure 11. For the particular arcs shown in Figure 10, both curves actually approach the same value, about 50dB at low frequencies. Since the constant voltage arc is longer in duration it begins to roll-off first.

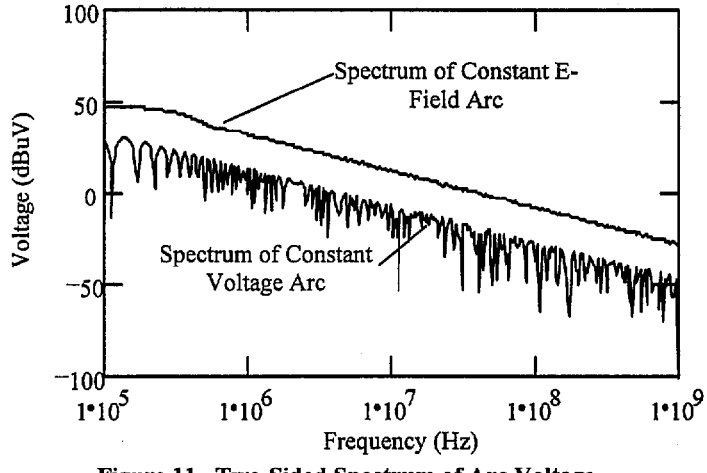

Figure 11. Two-Sided Spectrum of Arc Voltage

Calculation of Common Mode Current

The approximate antenna impedance for the test motor is shown in Figure 12. Due to the ideal nature of this equation, the impedance cycles between very distinct resonance points. Since the peak measured data was recorded for discrete bands, the calculated common mode current for each frequency band was constrained by the minimum impedance within the band. This helps remove some of the resonant effects. For simplicity, the current was computed at three points within each band. The minimum impedance of the three points in each band is plotted in Figure 12.

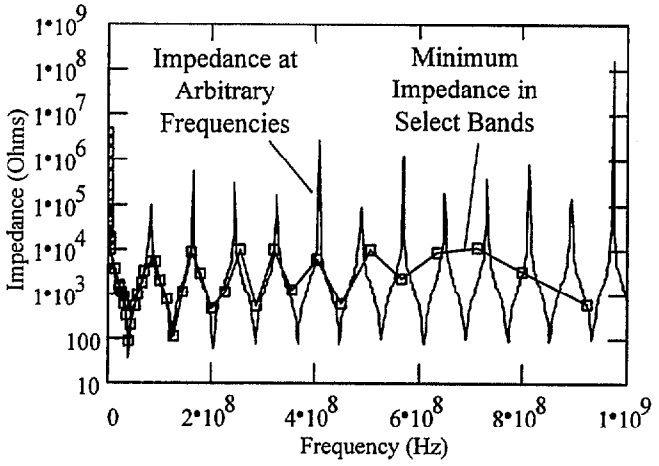

Figure 12. Predicted Wiring Harness Impedance

A network analyzer was used to measure the impedance between the motor housing and the wiring harness. A comparison between the measured data in Figure 13 and the predicted impedance in Figure 12 shows the actual impedance to be generally lower with fewer distinct resonant points. A more accurate prediction of the impedance would be difficult without a numerical field solution for the specific wiring and motor geometry. The inaccuracy in the wiring harness impedance along with the inability to accurately represent the arc impedance are major sources of error in the predictions.

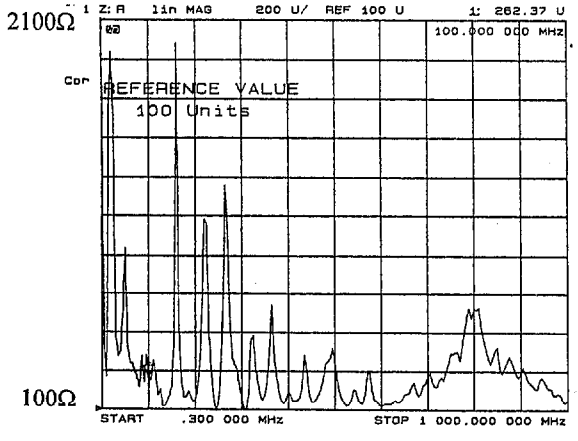

Figure 13. Measured Wiring Harness to Case Impedance

Using the calculated impedance and the two arc representations, the common mode current was calculated as shown in Figure 14. The prediction for the constant E-field arc is closest to the measured current. In general the constant voltage arc results in lower than measured common mode current while the constant E-field arc results in higher than measured current. This could be the result of inaccurate implementation of the arc resistance or may reflect the nature of the arcing.

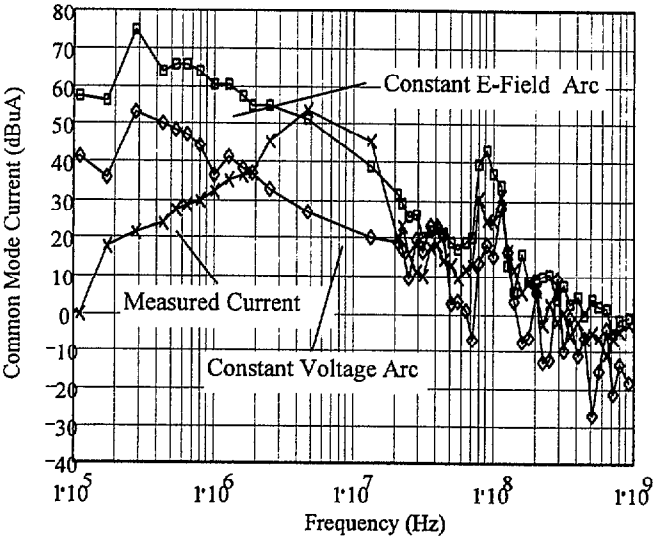

Figure 14. Measured vs. Predicted Common Mode Current

Calculation of Radiated Electric Field

The predicted radiated emissions were calculated at three points within each frequency band for the constant voltage arc and the constant E-field arc. These points are plotted on the graphs in Figures 15 and 16. Since the spectrum analyzer was in a peak hold mode, the highest value predicted in each interval should correspond to the measured emissions. Both spectrum analyzer and computed values are shown in RMS.

The radiated emissions comparison closely mimics the comparison of common mode current shown in Figure 14. The constant E-field arc results in higher levels and the constant voltage model results in lower levels. Large magnitude fluctuations in both models show the effects of wiring harness impedance and antenna resonance between 100MHz to 1GHz, but an envelope along the peaks of these curves follows the measurements fairly well. For the frequencies between 20 and 100MHZ, the constant voltage arc model is a closer approximation than the constant E-field arc. In this range the constant voltage arc is within about 6dB of measurements while the constant E-field arc deviates substantially. This discrepancy is intriguing, because the common mode current approximation in Figure 14 shows that the current from the constant voltage arc is no more accurate than the predicted constant value E-field arc approximation.

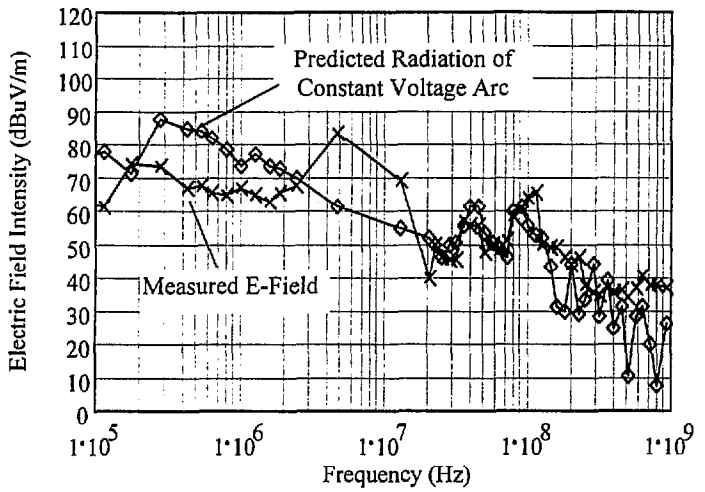

Figure 15. Comparison of Radiation for Constant Voltage Arc

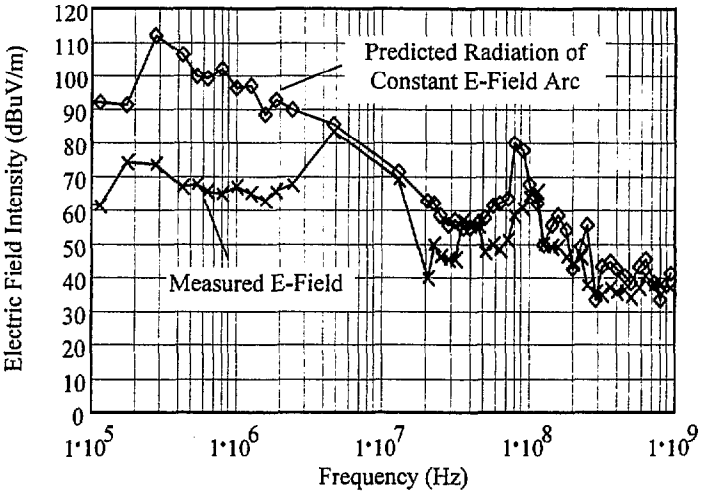

Figure 16. Comparison of Radiation for Constant E-Field Arc

FUTURE RESEARCH

Improvement to the computed wiring harness impedance and antenna characteristics can be accomplished using a variety of numerical methods including method of moments and finite element modeling. Use of these methods could provide more accurate input to the existing model but can not represent the time varying arc resistance. Improvement in the treatment of the arc resistance is certainly a suitable subject for further investigation. Since the time dependency of the arc voltage and resistance can be determined, the use of a finite difference time domain model to predict the motor radiation would be appropriate. Additional work to extend the analysis to lower frequencies is also of interest

REFERENCES

[1] A. Tustin and H. Ward, "The E.M.F.s Induced in the Armature Coils of D.C. Machines During Commutation," IEE Monograph No. 5111 U, April 1962.

[2] C. R. Suriano, "A Study of DC Permanent Magnet Motor Noise Related to Line Current," Master's Thesis, Purdue University, 1994.

[3] John R. Suriano, "Modeling of Electromechanical and Electromagnetic Disturbances in DC Motors," *1989 IEEE National Symposium on Electromagnetic Compatibility*, Denver, May 23-25 1989, pp. 258-262.

[4] Ragnar Holm, "Theory of Sparking During Commutation on Dynamos," Conference Record-AIEE IAS Annual Meeting, December 1962, pp. 588-595.

[5] K. Padmanabhan, A. Srinivsan, "Some Important Aspects in the Phenomenon of Commutator Sparking," *IEEE Transactions* , PAS, Vol. 84, May 1965, pp. 396-404.

[6] A. Srinivasan, K. Padmanabhan, "The Theory of Contact-Layer Behavior under a Commutating Brush," *IEEE Transactions*, PAS, Vol. 85, No. 2, pp. 132-140.

[7] D. P. Motter, "Commutation of D-C Machines and Its Effects on Radio Influence Voltage Generation," *AIEE Transactions*, Vol. 68, 1949, pp. 491-496.

[8] J. Sach and H. Schmeer, "Computer Aided Analysis of RFI Voltage Generation by Small Commutator Motors," *Symposium and Technical Exhibition on Electromagnetic Compatibility* No. 6, Zurich, 1985, pp. 551-556.

[9] Clayton R. Paul, *Introduction to Electromagnetic Compatibility*, John Wiley & Sons, New York, 1992.

[10] Elmer E. Bucher, *Practical Wireless Telegraphy*, Wireless Press, Inc., 1917.

[11] W. L. Weeks, *Antenna Engineering*, McGraw-Hill Book Co., New York, 1968. pp. 156,159.